

Development of EPA OTM 10 for Landfill Applications

Eben D. Thoma¹; Roger B; Green²; Gary R; Hater³;

C. Doug Goldsmith⁴; Nathan D. Swan⁵; Mike J. Chase⁶; and Ram A. Hashmonay⁷

ABSTRACT:

In 2006, the U.S. Environmental Protection Agency posted a new test method on its website called OTM 10 which describes direct measurement of pollutant mass emission flux from area sources using ground-based optical remote sensing. The method has validated application to relatively small, bounded area sources but additional guidance is needed for large area sources, such as landfills, where the emission zone can exceed the size of optical configuration leading to difficulties in relating measured fluxes to emissions per unit area. This paper presents the findings of a series of tracer release experiments conducted by U.S. EPA and Waste Management designed to improve the understanding of OTM 10 in landfill applications. OTM 10 plume capture efficiency data acquired at a variety of landfill sites under a range of meteorological conditions and measurement configurations are presented.

Experiments indicate an overall capture efficiency factor of 0.81 with a standard deviation of 0.33. Lower capture efficiencies from side slope releases are noted (0.69).

The combined data set is analyzed for factors influencing capture efficiency. A multiple linear regression is used to model the capture efficiency as a function of primary parameters including distance of the tracer release from the observing plane and wind speed. A simplified model based on the regression analysis is described and its use for approximating the area contributing to flux is presented.

¹ Research Environmental Scientist, Office of Research and Development, National Risk Management Research Laboratory, U.S. EPA, 109 TW Alexander Drive, E343-02, RTP, NC 27711, USA (corresponding author). E-mail: thoma.eben@epa.gov

² Senior Scientist, Waste Management, 2956 Montana Ave., Cincinnati, OH 45211. E-mail: rgreen2@wm.com

³ Senior Director of the Bioreactor, BioSite & New Technologies Office, Waste Management, 2956 Montana Ave., Cincinnati, OH 45211. E-mail: gwater@wm.com

⁴ Principal, Alternative Natural Technologies, Inc., 1847 Whittaker Hollow Road, Blacksburg, Virginia 24060. E-mail: dougg@infionline.net

⁵ Principal, Cygnus Environmental Group, 1944 Roanoke Ave., Louisville, KY 40205. E-mail: nathan_swan@yahoo.com

⁶ Staff Scientist, ARCADIS Inc., 4915 Prospectus Drive, Suite F, Durham, NC 27713. E-mail: mchase@arcadis-us.com

⁷ Principal Consultant, ENVIRON International Corporation, Chapel Hill NC. E-mail: rhashmonay@environcorp.com

INTRODUCTION

Quantification of fugitive methane emissions from landfills is of growing interest, not only from an anthropogenic source standpoint, but also as gas recovery and operation metrics for facility managers. Due to the large spatial extent and heterogeneous nature of landfill gas emissions, assessment of fugitive loss using traditional point sampling methods can be difficult (Börjesson et al. 2000; Spokas et al. 2003) which is leading to the investigation of alternate measurement approaches (Babilotte, et al 2008; U.S.

EPA, 2007). One such approach was developed by the U.S. Environmental Protection Agency (U.S. EPA) in conjunction with ARCADIS and centers on use of ground-based optical remote sensing (ORS) which provides improved sampling capability for heterogeneous area sources compared to point monitoring approaches. Posted on U.S. EPA's Emission Measurement Center website in 2006, Other Test Method 10 (OTM 10) "Optical remote sensing for emission characterization from non-point sources" describes direct measurement of pollutant mass emission flux from area sources using various ORS techniques. The approach, illustrated in Figure 1, utilizes open-path spectroscopic instrumentation to obtain path-integrated concentration (PIC) information along multiple plane-configured optical paths forming a virtual flux plane (OTM 10 plane) down wind from the area source. The multi-path pollutant concentration data along with wind vector information are processed with the Vertical Radial Plume Mapping (VRPM) algorithm to yield a mass emission flux for the source (Hashmonay and Yost, 1999; Thoma et al. 2005; U.S EPA 2006; Hashmonay et al. 2008).

For ideal area source measurement applications, the primary emission zone is spatially well-defined, relatively small in comparison to the OTM 10 plane (< 75% of plane length) and located in close proximity to the OTM 10 plane (outside source boundary distance < 75% of plane length upwind). Under these conditions, within specified wind speed and direction limits, all emissions are reasonably assumed to be advected through the OTM 10 observation plane leading to an accurate assessment of mass emission flux from the source. Previous tracer release studies support this assumption

with time-averaged emission flux measurement accuracies within 15% of actual for typical use conditions (Hashmonay et al. 2001; U.S. EPA. 2004a; Varma et al. 2005; U.S. EPA 2007) with underestimation in mass emission flux evident in cases of highly unstable atmospheric conditions (wind speeds < 1.0 m/s).

Frequently for landfill measurement applications, the emission area can be much larger than the OTM 10 optical configuration. Under these conditions, the emission area sampled by the OTM 10 measurement is difficult to define. Emission areas close to and centered on the OTM 10 plane will be robustly captured by the measurement configuration. Emission areas remote to the OTM 10 plane will be sampled less efficiently as the transported plume will have a progressively decreasing probability of passing through the optical configuration with increasing distance due to wind direction variance and turbulent dispersion. This loss in sampling efficiency does not invalidate the mass emission flux measurement but complicates accurate assignment of the area contributing to the emissions. Since area source emission factors can be expressed as emissions per unit area, understanding the area contributing to flux (ACF) measured with OTM 10 for large area sources is an important concern. This knowledge is also needed to allow meaningful comparisons between different area source measurement approaches.

To help address this issue, the U.S. EPA and Waste Management conducted a series of tracer release experiments at a variety of landfill sites. Experiment locations and dates included: Chapel Hill, NC (June 2006); Louisville, KY (Nov. 2007, March 2008, Jan.

2009); Lancaster, CA (Jan. 2008); Kirby, CA (Jan. 2008, June 2008); Tricites, CA (Feb. 2008, June 2008); Atascocita, TX (Feb. 2008); Maplewood, VA (March 2008, Sept. 2008); and Metro WI (May 2008, Oct. 2008). The goals of the collaboration were to provide additional technique validation and useful information for landfill deployments and to test various OTM 10 configurations allowing best use practices to be established (Thoma et al. 2008a, Thoma et al. 2008b). This paper focuses on the expanded OTM 10 method validation results and analysis of factors affecting the ACF for large area source applications. Following a description of the tracer release experiment methods and data analysis approaches, measurement results are presented and then analyzed for factors affecting the capture efficiency. This analysis is followed by description of a simplified model for estimation of ACF including uncertainties.

METHODS

Experiment Description

The experimental approach was based on comparison of the OTM 10-measured tracer release flux to the known tracer release rate to establish a capture efficiency factor (CEF) for the measurement. The experiments utilized metered gas releases of acetylene (C₂H₂) gas (99.8% purity, balance air, atomic absorption grade) or 99.9% pure methane from 10 to 30 meter size area release and point release configurations set up at various locations upwind of the OTM 10 optical plane with PIC data measured by open-path Fourier transform infrared spectrometers or open-path tunable diode lasers (TDLs). For the simulated area releases, the lateral dimension of the release area ranged from 3% to 17% of the OTM 10 plane length with an average value of 7% of

the plane length. The release rate of the tracer gas was controlled using calibrated mass flow controllers (EnviroNics Series 2000 or Alicat Scientific MC Series 16-Bit MFC) with pre and post cylinder weights recorded to double-check release rates. A standard OTM optical configuration was employed with the flux plane defined by five retro-reflecting mirrors as indicated in Figure 1. Three ground-level retroreflectors were used with the furthest defining the OTM 10 plane length. Two intermediate retroreflectors were located at approximately 1/3, and 2/3 of the full optical path length. The remaining two retroreflectors were located at the position of furthest ground retroreflector and were elevated by attaching to the midpoint and top of a scissor lift at approximately 6 m and 12 m heights respectively.

The dwell time for acquisition of the PIC data ranged from 20 to 30 seconds per beam path. Each of the five beam paths were sequentially scanned yielding complete cycle times of approximately 2.5 to 4 minutes. Each measurement consisted of a moving average of five successive cycles indicating an approximate 15 minute observation time for each experiment entry. Wind information was acquired using calibrated R.M. Young Model 05103 meteorological heads located at approximately 2 m and 14 m above the ground. Additional details of the tracer release experiments are contained elsewhere (U.S. EPA 2007, Thoma et al. 2008a, Thoma et al. 2008b, Waste Management-Veolia 2009).

Analytical Method

The EPA OTM 10 VRPM method was used for calculation of the tracer release emission. The computational algorithm utilizes a two-phase smooth basis function minimization (SBFM) approach for plume reconstruction where a one-dimensional SBFM reconstruction procedure is first applied in order to reconstruct the smoothed ground level and crosswind concentration profile. Then, the reconstructed parameters are substituted into the bivariate Gaussian function before applying the two-dimensional SBFM procedure, as described below and in U.S. EPA 2006.

In the first phase, a univariate Gaussian function is fitted to measured PIC ground level values. The error function for the minimization procedure is the Sum of Squared Errors (SSE) function and it is defined in the one dimensional SBFM approach as follows:

$$SSE(B, m_y, \sigma_y) = \sum_i \left(PIC_i - \sum_j \frac{B}{\sqrt{2\pi}\sigma_y} \int_0^{r_i} \exp\left[-\frac{1}{2}\left(\frac{m_y - r}{\sigma_y}\right)^2\right] dr \right)^2 \quad (1)$$

Where B is equal to the area under the one dimensional Gaussian distribution (integrated concentration), r_i is the pathlength of the i^{th} beam, m_y is the mean (peak location) and σ_y is the standard deviation of the Gaussian function. PIC_i is the measured path integrated concentration value of the i^{th} path. The Nelder-Mead simplex algorithm (Press et al. 1992) is used to retrieve the unknown parameters.

When applying the second phase of the two-phase process, substituting the standard deviation and peak location retrieved in the one-dimensional SBFM procedure into a

reduced (the vertical peak location is assumed at the ground level and the correlation coefficient is equal to zero) bivariate Gaussian function yields:

$$G(A, \sigma_z) = \frac{A}{2\pi\sigma_{y-1D}\sigma_z} \exp\left\{-\frac{1}{2}\left[\frac{(r \cdot \cos \theta - m_{y-1D})^2}{\sigma_{y-1D}^2} + \frac{(r \cdot \sin \theta)^2}{\sigma_z^2}\right]\right\} \quad (2)$$

Where σ_{y-1D} and m_{y-1D} are the standard deviation and peak location respectively along the crosswind direction that are found in the one-dimensional SBFM procedure; A is a normalizing coefficient which adjusts for the peak value of the bivariate surface; and σ_z is standard deviations in the vertical direction. To fit the unknown parameters of the smooth basis function to the PIC data, an error function for minimization has to be defined also for this phase. The SSE function for the second phase is defined as:

$$SSE(A, \sigma_z) = \sum_i \left(PIC_i - \int_0^{r_i} G(r_i, \theta_i, A, \sigma_z) dr \right)^2 \quad (3)$$

Where PIC represents the measured PIC values and the index i represents the different beams. The SSE function is minimized using the Nelder-Mead simplex method to solve for the two unknown parameters.

Once the parameters of the function are found for a specific run, the concentration values for every square elementary unit in a vertical domain are calculated. These values are then integrated, incorporating wind speed data at each height level to compute the flux. In standard application, the wind speed data at each height level is calculated through a linear interpolation process using two wind speed measurements at approximately 2 m and 14 m vertical locations. For this work, a standard 20 m vertical integration height is used for the flux calculation. In this stage, the

concentration values are converted from parts per million by volume to grams per cubic meter, considering the molecular weight of the target gas and ambient temperature. This enables the flux in grams per second through the OTM 10 plane to be directly calculated, using the component of wind speed in meters per second as illustrated in the following equation:

$$\text{Flux (g/s)} = [\text{IC (g/m)}] [\text{wind speed (m/s)}] [\cos (\text{wind direction})] \quad (4)$$

Where:

IC= the integrated concentration over the vertical plane area

and $\cos (\text{wind direction})$ yields the wind speed component normal to the OTM 10 plane.

Each OTM 10 flux calculation in this data set represents a moving average of 5 successive VRPM measurements cycles. This is done to reduced noise in the calculation as described in Varma et al. 2005. A 5-cycle average is recommended for general OTM 10 applications. Standard OTM 10 QA criteria are employed to select valid results (U.S. EPA 2006) with concordance correlation factor data quality indicator values above 0.80 used.

Database Description

As of January 2009, the tracer-release database consists of 1440 entries of which a subset of 1161 values are utilized in the current analysis of OTM 10 capture efficiency in the large area source use regime. In this scenario, the potential emission zone of the area source is much larger than the OTM 10 plane length so horizontal capture loss

effects are less important as the area contributing to the measured flux exceeds the OTM 10 foot print in the lateral dimension under normal wind variance. To properly represent this aspect, the analysis is restricted to tracer release results that are well-centered on the OTM 10 plane. For these tracer release trails, the lateral extent of the release area is small in comparison to the OTM 10 plane length (average value of 7% of plane length) and the release point is in some cases located outside of the boundaries of the OTM 10 plane dimensions. The position of the release is such that the prevailing wind direction during the experiment transports the plume to the OTM 10 plane thereby insuring adequate plume capture. A wind vector calculation is used to determine the intersection point of the plume center and the OTM 10 plane for each of the data set entries. Intersection points near the edge of the optical configuration (< 20% and > 80% of the OTM 10 plane length), are excluded from the following analysis (245 values). It is noted that these edge intersection points exhibit significantly lower capture due to horizontal loss and their inclusion would be relevant in an analysis capture efficacy for small bounded area sources in which case the relative size of the OTM 10 plane length in comparison to the source size becomes a key factor. Releases approaching the OTM 10 plane at oblique angles (> 60° from normal) are also excluded (19 values) as they exhibit atypically low capture efficiencies and high uncertainty in lateral plume capture. Additionally, 15 outlier values (1.3%) were removed from the data set using the ROUT method on a linear regression fit of capture efficiency vs. release distance with Q coefficient at 2% (Motulsky et al. 2006) using GraphPad Prism ver 5 (GraphPad Software, La Jolla, CA,

USA). The outlier CEF values ranged from 1.52 at WARD = 221m to 2.85 at WARD = 63 m.

The database consists of 61 different release experiments using 24 different OTM 10 optical configurations and 22 release rates. Release from horizontal flat surfaces, such as the top of the landfill account for 48 of the experiments whereas releases from the landfill side slopes account for the remaining 13 experiments. Slope release experiments were executed with the OTM 10 plane located at the top of the landfill hill with winds coming up the slope toward the OTM 10 plane. Simulated area source releases make up 41 of the surface release experiments and 11 of the slope release experiments with the remaining executed as point releases. Nine of the surface release experiments (Louisville KY, Jan. 2009) were conducted at a non-landfill field site which provided large open space facilitating long release geometries. The average number of data points per experiment is 19.0 with a standard deviation (σ) of 21.8, with a minimum number of entries of 1, and a maximum of 103. Considering individual results, surface, slope, area, and point releases account for 88%, 12%, 86%, and 14 % of the data respectively. Acetylene releases account for 49.2 % of the data with methane releases making up the remainder. In all cases, pre-release concentrations of acetylene were far below instrument detection limits so no background correction for the tracer flux measurement was required. The methane release experiments were conducted in areas away from primary landfill emissions or at non landfill sites to avoid large methane background fluctuations during the tracer measurement. Methane background concentrations ranged from was 1.84 ppm to 2.43

ppm. Background methane concentrations were measured for each beam path for approximately 15 minutes before and after each methane release and the average value of these measurements was subtracted from measured values during the release for each path to compensate for the background methane flux. The data set includes a representative range of typically encountered meteorological conditions with the majority of the experiments conducted under Pasquill stability classes B and C. To aid in comparison across data sets, all geometric parameters are defined with respect to the observing OTM 10 plane. Wind angle (WA) is defined as the absolute value of the angle between the average wind direction for the measured set and a perpendicular vector to the OTM 10 plane. The wind-adjusted release distance (WARD) is equal to the perpendicular distance of the release point to the OTM plane divided by the cosine of WA and represents the distance traveled by the release plume to the observation plane. For simulated area source experiments, the release point is defined as the center of the release area. The wind speed (WS) parameter represents a linear interpolation of values measured at 2 m and 14 m as part of standard OTM 10 procedure.

RESULTS AND DISCUSSION

Combined Results

Tracer release experiment data are summarized in Table 1. The majority of experiments were conducted in the typically encountered 2 m/s to 4 m/s WS range. The range of WA exceeds normal OTM 10 use limits ($\pm 30^\circ$ from normal) however, as previously discussed, this data set includes a vector calculation ensuring well-centered plume intersection. This extended WA range is appropriate when considering OTM 10

performance in large area source applications were the emission zone exceeds the primary footprint of the sampling configuration at non-normal wind angles. The dataset covers a range of OTM 10 plane lengths with an average value of 153.3 m with the majority of values between 100 and 200 m. The WARD ranged from very close release points (8.1 m) to very far release points (289.2 m) with an average of 66.3 m. Utilized release rates cover a range from 0.11 g/s to 6.53 g/s with no observed effect on CEF. The average CEF values for several release rate ranges are: 0.91 ($\sigma = 0.38$), 0.79 ($\sigma = 0.22$), 0.83 ($\sigma = 0.20$), 0.83 ($\sigma = 0.13$) for release rates <1 g/s, 1-2 g/s, 3-5 g/s and >5 g/s respectively with these comparisons considering only WARD values < 100m to avoid distance effects. The overall average CEF value for the combined dataset is 0.81 ($\sigma = 0.33$). This includes the affects of reduced CEF at large WARD values.

In addition to a combined summary, Table 1 presents results separated by release location (surface or slope) and release type (area or point). Due to the large standard deviation in the data, differences in CEF values for the different release locations and types are difficult to assess with confidence. Releases from slope locations have a slightly lower overall average CEF value (0.69) compared to surface releases (0.83) which may be expected since slope release likely experience additional dispersive turbulence due to encountered topography. Little difference in overall average CEF values are seen when comparing point releases (0.80) to simulated area releases (0.81). There was no observed dependency of CEF on tracer release gas type.

Figure 2 displays a histogram of CEF values for the combined dataset with a highest number of occurrence around CEF = 0.75. Large overestimation of release rate ($> 2\sigma$ from mean, CEF > 1.48) was observed in 4.1% of the readings and with values distributed throughout the experiment sets with more frequent occurrence at mid to high wind speeds with release locations close to the OTM 10 plane. Extreme underestimation in release rate ($< 30\%$ of actual) accounted for 5.3% of the values with a proportionately greater occurrence at long release distances. It is noted that for typical use scenarios, average measurement values over extended time periods are usually employed which can greatly reduced the impact of extreme values.

CEF Dependence on Plume Transport Distance and Wind Speed

Figure 3 investigates the trend to lower CEF values with increasing distance from the OTM 10 plane by plotting the CEF vs. WARD for individual values of the combined data set. The evident reduction in capture efficiency is expected as the transported plume experiences a progressively decreasing probability of passing completely through the optical configuration with increasing distance due wind direction variance and turbulent dispersion. A linear regression fit is shown with y-axis intercept = 1.02 and correlation coefficient $r^2 = 0.17$. The low correlation coefficient in the combined data set is due primarily to random data scatter however a systematic variation with wind speed and differences in release location contributes to the spread in data. It is noted that the CEF results are not strongly dependent on the intersection point of the plume center with the VRPM plane for this dataset as intersection points near the edge of the optical configuration ($< 20\%$ and $> 80\%$ of the OTM 10 plane length), are

excluded from the analysis. The average CEF values of results with plume intersections occurring at 20% to 39%, 40% to 59%, and 60% to 80% of the OTM plane length are 0.82 ($\sigma = 0.51$), 0.83 ($\sigma = 0.30$), 0.81 ($\sigma = 0.32$), respectively with the largest standard deviation ($\sigma = 0.51$) occurring for the group closest to the open path instrument where the optical beams have the least vertical separation.

This figure is presented to show the distribution in data points as a function of WARD for the tracer release experiments and additionally to illustrate the general variability in the data. There is a high concentration of release values at WARD locations less than 100 m due primarily to the difficulty in execution of well centered releases at long distances. With regard to scatter, tracer release data typically exhibit an exaggerated variability compared to actual area source measurement data as a consequence of non-optimal overlap of the relatively small simulated area or point source release plume with the optical sampling beam geometry. For example, a plume which is small in spatial extent may not intersect all three vertical optical beams in a stable fashion resulting in additional variability in the OTM 10 VRPM algorithm output.

Additionally, for optimal results, a plume measured by OTM 10 should overlap multiple optical path elements in the horizontal direction. A laterally underdeveloped release plume may not cross the OTM 10 plane with sufficient overlap on multiple ground-level beam paths. This case can lead to significant underestimation (-30%) or overestimation (+190%) of the flux due calculation degeneracy in the OTM 10 VRPM algorithm (Hashmonay and Yost, 1999; Abichou et al. 2009). These factors are usually not an issue with larger area source measurements but may contribute to the

observed CEF variability for small area and point tracer release experiments, especially in cases where the release position is in close proximity to the OTM 10 plane so the plume has less time to spatially develop. In general, extended source observation times under stable wind conditions (at least 2 hours), are recommended as this will help reduce variability will produce a more reliable average mass emission flux estimation.

Figure 4 plots CEF vs. wind speed for the combined data set. For ease of viewing, data is binned in 1 m/s increments with bin average and $\pm 1 \sigma$ shown. An increase in CEF with wind speed is evident in the binned linear regression with a correlation coefficient $r^2 = 0.96$. Part of the observed dependence is due to more efficient plume capture at higher wind speeds as atmospheric stability generally increases. It is noted that a nonlinear fall-off to zero CEF is expected as wind speeds approach zero so the linear fit, and y-axis intercept, of Figure 4 does not represent actual results at very low wind speeds. The OTM 10 method is known to significantly underestimate emissions at very low wind speeds (< 1 m/s) in unstable atmospheric condition (Class A) and is not recommend for use under these conditions.

It is instructive to investigate the dependence of CEF on WARD with data values grouped by tracer release experiment as shown in Figure 5, which presents 52 of the 61 total experiments possessing three or greater individual results. These data consist of 40 surface release experiments (30 area, 10 point) and the 12 slope release experiments (10 area, 2 point). Simulated area releases and point release are combined in this

figure since the averages, ranges, and standard deviations of the data are very similar (Table 1). Each data point of Figure 5 is equally weighted. The average number of data points per experiment is 22.1 ($\sigma = 22.2$) with a minimum of three (3) and a maximum of 103. Since each experiment was conducted over a relatively short time period (30 minutes to 2 hours), the wind speed was relatively constant during the experiment. The experiment average WS values ranging from 1.5 m/s to 7.7 m/s with an overall data set mean of 3.3 m/s. A linear regression fit to the data is also shown ($r^2 = 0.39$). The y-axis intercept and slope are similar to the combined analysis (Figure 3), with the improvement in correlation coefficient a consequence of reduced scatter by averaging. The similarity in the linear fit of experiment-grouped and combined analysis (Figure 3) provides some confidence in the weighted regression model approach described in the following section. Significant intra-experiment variability in the WARD and CEF parameters is evident in the experiment-grouped results with the error bars represent ± 1 standard deviation in results. As previously discussed, some of the variability in CEF for releases close to the OTM 10 plane is likely due to non optimal overlap of the release plume with the optical paths for plumes which may be small in spatial extent. These effects can lead to both overestimation and underestimation of the flux however these factors tend to cancel providing a more stable and accurate experiment average if sufficient sampling time is employed.

A comparison of release experiment locations (Figure 5) shows somewhat lower CEF for slope releases (avg. = 0.71, $\sigma = 0.28$) compared to surface releases (avg. = 0.87, $\sigma = 0.27$) where the surface average is limited to WARD locations less than 124 m to allow

similar comparisons by excluding the effect of CEF reduction with increasing WARD. This observation, also noted in the combined summary (Table 1), is likely a consequence of additional vertical dispersive turbulence due to encountered topography for slope releases. Due to the lack of slope release data at large WARD, a separate analysis of CEF reduction as a function of release distance from the OTM 10 plane is not currently warranted but is the subject of potential future work. It is likely that the CEF fall-off with distance will be significantly greater for slope measurements compared to horizontal surface measurements.

Figure 5 additionally displays experiments with average WS greater than 5 m/s (N=9). As discussed in Figure 4, an increase in CEF with WS is evident and partially explained by more efficient plume capture at higher wind speeds as atmospheric stability generally increases. Figure 5 shows that high WS entries may account for a disproportionate percentage of results which overestimate CEF at WARD < 100 m. This effect may in part be due to increased potential for non-optimal overlap with the optical beams as the tracer release plume has less ability to disperse before interacting the OTM 10 plane. It is also possible that a slight WS bias exists in the OTM 10 method. This was not observed in previous OTM 10 validation studies but the current data set reflects a significantly larger range in WS values.

Estimation of Area Contributing to Flux for Horizontal Surfaces

As previously discussed, a central issue for use of EPA Method OTM 10 for large area source applications relates to the estimation of the area contributing to flux (ACF).

Any definition of ACF must be based on estimations of CEF reduction as a function of significant variables. Based on the presented composite dataset, a simplified model of CEF fall-off as a function of two primary variables (WARD and WS) is presented. This simplified model is then used as basis for a definition of ACF which can be useful for large area source OTM 10 measurement applications when tracer release plume capture data quality indicators are not actively employed. Currently, the OTM 10 method does not require use of tracer releases to inform plume capture. The addition of tracer releases to an OTM 10 test design would improve knowledge of capture efficiency for a specific configuration and meteorological condition however these measures can add significant expense and potential environmental impact to the assessment so are not recommend for continuous use in conjunction with OTM 10. As shown previously, the CEF is dependent on both WARD and WS. To decouple the effects of these parameters on CEF, a multiple linear regression is utilized on a weighted average of experiment-grouped results. This analysis is limited to surface release experiments since slope release results at large WARD are not sufficiently represented for robust analysis. The following multiple linear regression (Eq. 5) is found when considering all surface release experiments (N=48) weighted by number of results per experiment:

$$\text{CEF} = 0.712 - 3.10 \times 10^{-3} (\text{WARD}) + 0.102 (\text{WS}) \quad (5)$$

The r^2 value for the multiple linear regression is 0.60 with standard error coefficients of 6.68×10^{-2} , 5.10×10^{-4} , and 1.77×10^{-2} for the coefficient, WARD and WS predictors

respectively with p-values for all predictors < 0.001 which shows that they are significant. The model accounts for 60% of the observed variability in the experimental dataset. This analysis was produced using Minitab ver. 15.1.30.0 (Minitab Inc., State College, PA, USA).

For area-related mass emission calculations (i.e., g/m^2 per unit time), a working definition of ACF for large area sources can be based on Eq. 5. At a given wind speed, the modeled CEF will fall linearly from an initial value to zero with increasing distance from the OTM 10 plane. An estimation of the mass captured by the OTM 10 measurement is found by multiplying the modeled CEF by the OTM 10-measured flux. This estimation can be expressed on a normalized percentage basis by starting at an assumed 100% mass capture in close proximity to the OTM 10 plane, falling to 0% mass capture with a slope determined by experiment WS. Figure 6 plots the fall-off in normalized captured mass as a function of distance from the OTM 10 plane at wind speeds of 2 m/s and 7 m/s with the secondary lines representing ± 1 standard error in the WARD slope coefficient. The x-axis intercept for the trend lines represent the points of 0% mass capture ($\text{CEF} = 0$) and occur at 295 m and 460 m for the 2 m/s and 7 m/s cases respectively.

Assuming a spatially uniform emission zone, the area under the captured mass curve (triangular region) of Figure 6 represents 50% of the total mass that would be measured assuming a step function fall-off in capture efficiency at the point of 0% mass capture. A definition of ACF that was based on the full distance to the point of

0% mass capture would significantly under estimate emissions per unit area. To obtain a more realistic estimate, it is reasonable to define the ACF as a product of the OTM 10 plane length multiplied by $\frac{1}{2}$ the distance to 0% mass capture. In this concept, actual emissions that originate beyond $\frac{1}{2}$ the distance to 0% mass capture would compensate for emissions not captured due to CEF fall-off at distances closer to the OTM 10 plane. For the data of Figure 6, a 150 m OTM plane length would yield ACFs of 22,125 m² for the 2 m/s wind speed case and 34,500 m² for the 7 m/s case.

It is noted that the default ACF estimate is derived from the ensemble dataset which covers a range of typically utilized OTM 10 plane lengths as described in Table 1 and associated text and is not recommended for use at extremely short OTM plane lengths (less than 75 m). An attempt was made to improve model performance by including estimates of atmospheric stability generated from observations acquired during the release experiments, however this did not significantly improve model prediction for this data set (r^2 increase to 0.62 from 0.60). This is likely due to the presence of wind speed as a parameter, which is an indirect indicator of atmospheric stability, coupled with the significant data variability, and lack of sufficient span in stability conditions over which the experiments were executed (predominantly class B and C). Highly unstable atmospheric conditions (Class A, WS < 1.0 m/s, high insolation) will undoubtedly reduce CEF as a function of WARD but these conditions are to be avoided in the preferred application of OTM 10. In a similar manner, highly stable atmospheric conditions will likely increase OTM 10 fetch but this is to first order accounted for in the wind speed parameter of the current simplified model with

subsequently discussed uncertainty. The current embodiment of OTM 10 does not include stability class estimation however this is likely an important consideration for large area source applications and should be considered as an area of future method development research.

The uncertainty in horizontal ACF model is estimated at $\pm 15\%$ based on the standard error of the WARD slope coefficient of Eq. 5. The overall measurement uncertainty expressed in emissions per unit area would include the ACF uncertainty in addition to uncertainty in the measured flux value, including concentration measurement uncertainty, which is estimated at $\pm 20\%$ using average experiment values when coupled with the indirect correction for overestimation of CEF at elevated wind speed using the normalized mass capture representation.

In practical landfill use, there will be occasions where the estimated CEF fall-off distance will extend beyond the horizontal terrain to the slope edge. In this situation, the CEF fall-off would likely differ from Eq. 5 as the slope emission plume dispersion are more complex. As discussed, the database is not sufficient for a standalone slope analysis much less a separate analysis of combined horizontal surface and slope cases however some insight can be gained by including the slope experiment averages ($N = 12$) with the surface experiments ($N = 48$). In this case the weighted multiple linear regression coefficients of Eq. 5 become 0.732, -3.34×10^{-3} , and 9.41×10^{-2} for the leading coefficient, WARD, and WS parameters respectively. The r^2 value is reduced

to 0.55 and the standard error becomes 6.51×10^{-2} , 5.15×10^{-4} , and 1.65×10^{-2} for the coefficient, WARD and WS predictors respectively with p-values for all predictors < 0.0001 . The model produced by combining the slope and surface data may be useful in estimating ACF for cases in which the sampling configuration includes a significant flat horizontal region adjacent to OTM 10 plane followed by a slope region located upwind of the flat region. The uncertainty in this estimate is expected to become progressively larger as the distance from the OTM 10 plane to the slope decreases. Selective use of tracer release validation during OTM 10 experiments can be used to provide additional confidence in CEF fall-off in case of mixed or complex topography.

SUMMARY

This paper presents recent tracer-release experiment results investigating the performance of EPA Method OTM 10 for applications where the emission zone is larger than the sampling plane length. The objective of the research was to provide additional validation data for the OTM 10 method and to investigate factors affecting the area contributing to flux for large area source applications. The experiments were conducted at a variety of landfill sites around the U.S. having varying local topography and surrounding ground cover. Experiments were executed under a typically encountered mix of meteorological conditions using a range of OTM 10 plane configurations. Release geometries included both point and area releases from flat horizontal surfaces and side slopes. The overall CEF value for the experiments was 0.81 with a standard deviation of 0.33 with lower capture efficiencies from slopes noted. The combined data set was analyzed for factors influencing CEF and a multiple

linear regression equation for approximating CEF fall-off as a function WARD and WS was presented. Based on this equation, a working definition of ACF along with estimation uncertainties was discussed.

DISCLAIMER

This article has been reviewed by the Office of Research & Development, U.S. EPA, and approved for publication. Approval does not signify that the contents necessarily reflect the views and policies of the agency nor does mention of trade names or commercial products constitute endorsement or recommendation for use. The research presented here was performed under Cooperative Research and Development Agreement #372-05 between the U.S. EPA and Waste Management. The U.S. EPA component of the effort was funded and managed under contract EP-C-04-023 (Work Assignment 4-13) with ARCADIS Inc. The work was performed under a U.S. EPA approved quality assurance project plan. The presented analysis was formulated, written, and quality assured by U.S. EPA personnel using data acquired by U.S. EPA contractors and project cooperators.

ACKNOWLEDGEMENTS

This work reflects the contributions of many individuals working within U.S. EPA, ARCADIS Inc. and Waste Management and its affiliates. In particular, the authors acknowledge the great efforts, Chris Johns, and Tom Pike in field data collection and collaboration with Antoine Babilotte of Veloia in the October Metro release study. Thanks to Mark Modrak and Eric Morris with ARCADIS for their efforts. Thanks to

Jeff Chanton of Florida State University, Mort Barlaz of NC State University and Sze Tan of Picarro for many helpful discussions. We appreciate the direction and support of Susan Thorneloe, Buddy Thompson, Shawn Lafferty, and Paul Groff with U.S. EPA's Office of Research and Development and Robin Segal, Jason DeWees, and Connie Sue Oldham with U.S. EPA's Office of Air Quality Planning and Standards.

REFERENCES

- Abichou, T., Clark, J., Tan, S., Chanton, J., Hater, G., Green, R., Goldsmith, D., Barlaz, M., and Swan, N. (2009), "Uncertainties associated with the use of OTM-10 to estimate surface emissions in landfill applications." Submitted to the Journal of the Air & Waste Management Association
- Babilotte, A., Lagier, T., Fianni, E., Taramini, V. (2008). "Fugitive methane emissions from landfills: a field comparison of five methods on a French landfill." *Proceedings of the Global Waste Management Symposium*, September 7-10, Cooper Mountain, CO.
- Börjesson, G., Danielsson, Å., Svensson, B. H. (2000). "Methane fluxes from a Swedish landfill determined by geostatistical treatment of static chamber measurements." *Environ. Sci. Technol.*, 34, 4404-4050.
- Hashmonay, R.A. and Yost, M.G. (1999) "Innovative approach for estimating fugitive gaseous fluxes using computed tomography and remote optical sensing techniques." *Atmos. Environ.*, 49, 966-972.
- Hashmonay, R.A., Natschke, D.F., Wagner, K., Harris, D.B., Thompson, E.L., Yost, M.G. (2001) "Field evaluation of a method for estimating gaseous fluxes from area

- sources using open-path Fourier transform infrared.” *Environ. Sci. Technol.*, 35 (11), 2309-2313.
- Hashmonay, R.A., Varma, R.M., Modrak, M.T., Kagann, R.H., Segall, R.R., Sullivan, P.D. (2008). “Radial Plume Mapping: A US EPA test method for area and fugitive source emission monitoring using optical remote sensing.” *Advanced Environmental Monitoring*, Springer Netherlands, 21-36.
- Motulsky, H.M., Brown R.E. (2006). “Detecting outliers when fitting data with nonlinear regression – a new method based on robust nonlinear regression and the false discovery rate.” *BMC Bioinformatics*, 7:123.
- Press, W.H., Teukolsky, S.A., Vetterling, W.T., and Flannery, B.P. (1992), *Numerical Recipes in FORTRAN: The Art of Scientific Computing*, (second ed.), Cambridge University Press, Cambridge, New York.
- Spokas, K., Graff, C., Morcet, M., Aran, C.(2003). “Implications of the spatial variability of landfill emission rates on geospatial analyses.” *Waste Management*, 23, 599-607.
- Thoma, E. D., Shores, R. C., Thompson, E. L., Harris, D. B., Thorneloe, S. A., Varma, R., Hashmonay, R. A.; Modrak, M. T., Natschke, D. F., Gamble, H.A. (2005) “Open path tunable diode laser absorption spectroscopy for acquisition of fugitive emission flux data.” *J. Air and Waste Manage. Assoc.* 55, 658-668.
- Thoma, E.D., Thorneloe, S.A., Segall, R.R., Green, R.B., Hater, G.R., Hashmonay, R.A., Modrak, M.T., Chase, M.J., Goldsmith, C.D. (2008). “Development of EPA OTM 10 for landfill applications, interim report 1.” *Proceedings of the 101st Annual Conference of the Air & Waste Management Association, June 24-27, Portland, OR.*

- Thoma, E.D., Thorneloe, S.A., Segall, R.R., Green, R.B., Hater, G.R., Hashmonay, R.A., Modrak, M.T., Chase, M.J., Goldsmith, C.D. (2008). "Development of EPA OTM 10 for landfill applications, interim report 2." *Proceedings of the Global Waste Management Symposium*, September 7-10, Cooper Mountain, CO.
- U.S. EPA. (2004a). "Measurements of fugitive emissions at region I landfill." U.S. EPA Report EPA-600/R-04-001, At Web Site:
<http://www.epa.gov/nrmrl/pubs/600r04001/600r04001.pdf>.
- U.S. EPA. (2004b). Evaluation of Former Landfill Site in Colorado Springs, Colorado Using Ground-Based Optical Remote Sensing Technology, U.S. Environmental Protection Agency Report EPA-600/R-05/-41 At Web Site
<http://www.epa.gov/ORD/NRMRL/pubs/600r05041/600r05041.htm> .
- U.S. EPA. (2006). EPA Test Method (OTM 10), "Optical Remote Sensing for Emission Characterization from non-point sources." U.S. EPA Technology Transfer Network Emission Measurement Center, Web Site;
<http://www.epa.gov/ttn/emc/prelim/otm10.pdf>.
- U.S. EPA. (2007). "Evaluation of Fugitive Emissions Using Ground-Based Optical Remote Sensing Technology." U.S. EPA Report EPA/600/R -07/032, At Web Site:
<http://www.epa.gov/nrmrl/pubs/600r07032/600r07032.pdf>.
- Varma, R., Hashmonay, R.A., Kagann, R., Bolch, M.A. (2005) "Optical Remote Sensing to Determine Strength of Non-Point Sources." ESTCP #CP-0241 Duke Forest Validation Study, AFRL Report AFRL-ML-TY-TR-2005-4584 At Web Site,
http://www.clu-in.org/download/char/voc2008/duke_forest.pdf

Waste Management-Veola. (2009) "Fugitive methane emissions from landfills: a field comparison of five methods on two U.S. landfills" In Preparation.

Figure and Table Captions

Figure 1: OTM 10 optical configuration for area source measurements.

Table 1: Combined summary of tracer release data (left columns) with data separated by release location and type (right columns).

Figure 2: Histogram of CEF values (N = 1161).

Figure 3: CEF vs. WARD for the combined data set.

Figure 4: CEF vs. WS for the combined data set with error bars indicating $\pm\sigma$ in CEF and wind speed for the y-axis and x-axis respectively.

Figure 5: CEF vs. WARD grouped by tracer release experiment with error bars indicating $\pm\sigma$ in CEF and WARD for the y-axis and x-axis respectively.

Figure 6: Estimate of normalized mass capture reduction as a function of distance from the OTM 10 plane based on multiple regression model of surface release experiments at 2 m/s and 7 m/s with shaded regions indicating ± 1 std. error in the WARD regression coefficient.

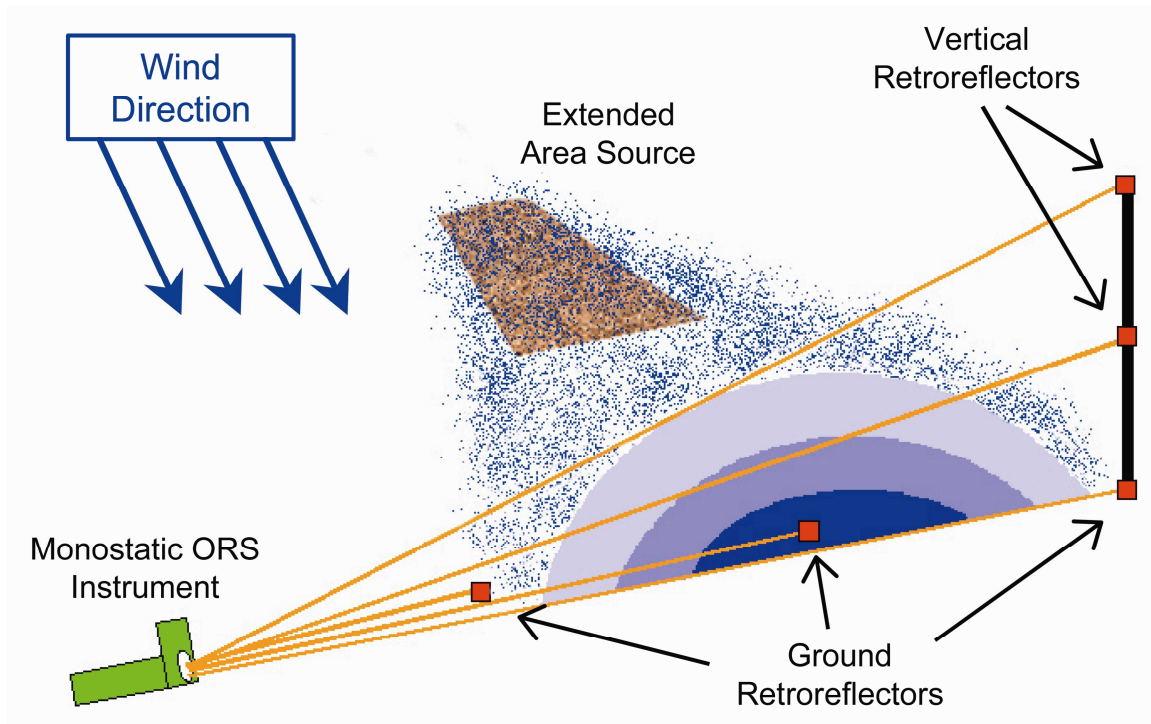


Fig 1

| | Release Rate (g/s) | Plane Length (m) | Wind Speed (m/s) | Wind Angle (deg) | WARD (m) | Overall CEF | Surface Release CEF | Slope Release CEF | Area Release CEF | Point Release CEF |
|--------|--------------------|------------------|------------------|------------------|----------|-------------|---------------------|-------------------|------------------|-------------------|
| Avg. | 1.37 | 153.3 | 3.2 | 27.8 | 66.3 | 0.81 | 0.83 | 0.69 | 0.81 | 0.80 |
| StdDev | 1.50 | 59.3 | 1.4 | 14.6 | 43.7 | 0.33 | 0.33 | 0.36 | 0.33 | 0.36 |
| Min | 0.11 | 56.0 | 0.7 | 0.0 | 8.1 | 0.00 | 0.00 | 0.24 | 0.03 | 0.00 |
| Max | 6.53 | 318.0 | 7.9 | 59.6 | 289.2 | 1.79 | 1.79 | 1.66 | 1.79 | 1.78 |
| N | 22 | 24 | 1161 | 1161 | 1161 | 1161 | 1023 | 138 | 999 | 162 |

Table 1

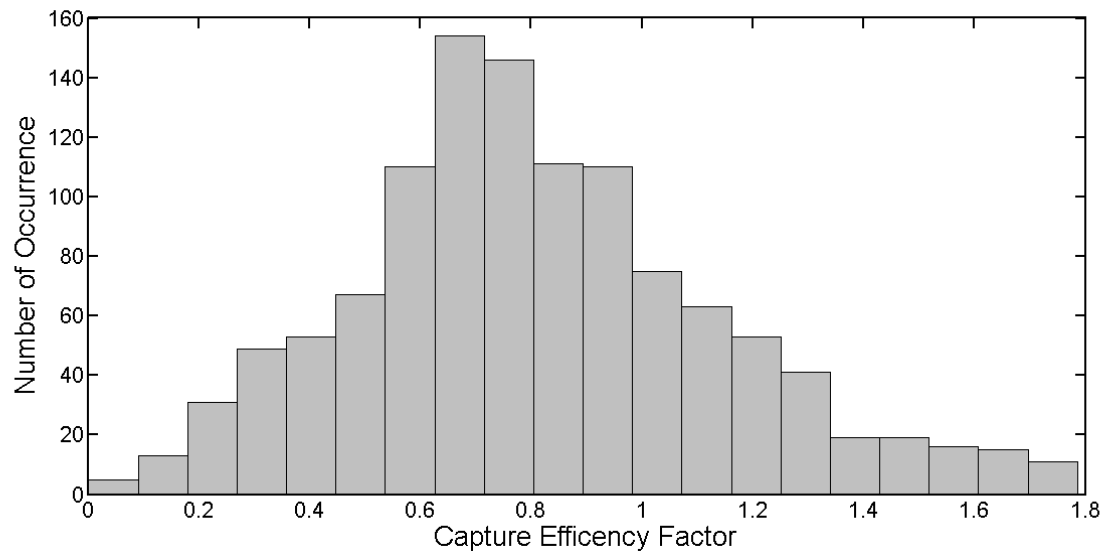


Fig. 2

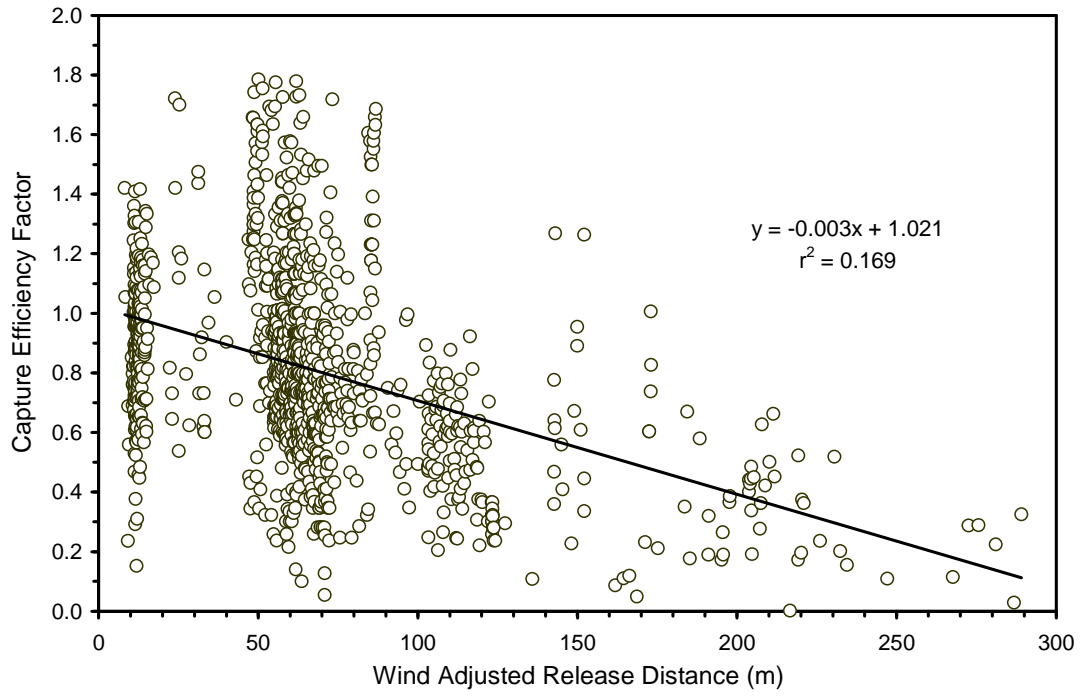


Fig. 3

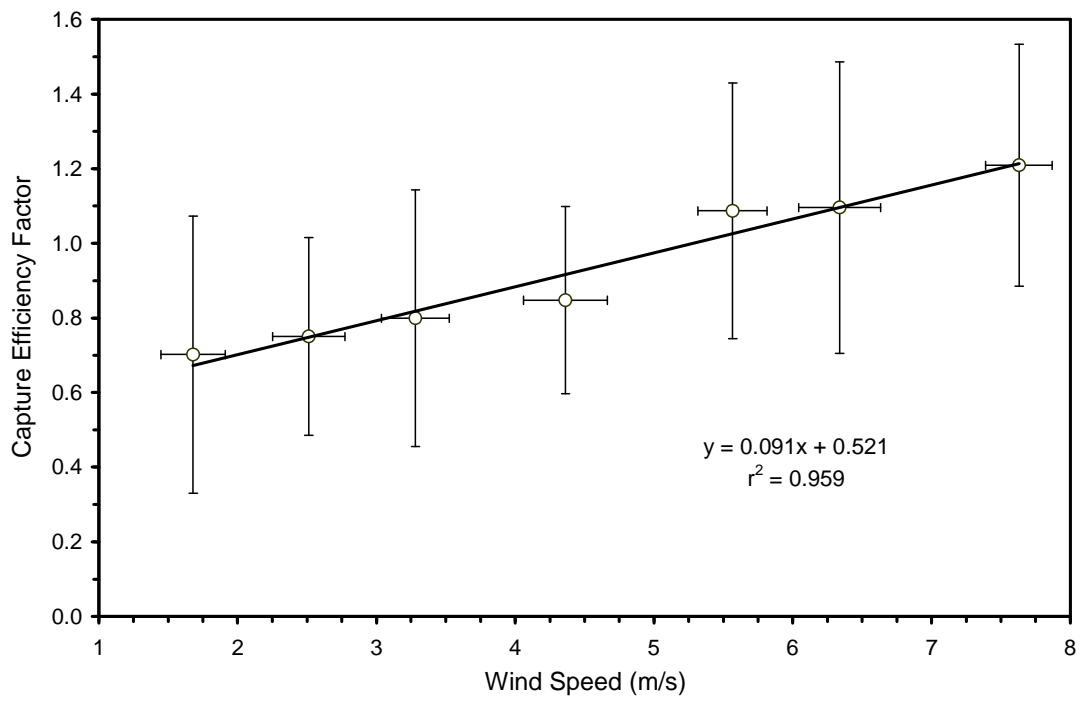


Fig. 4

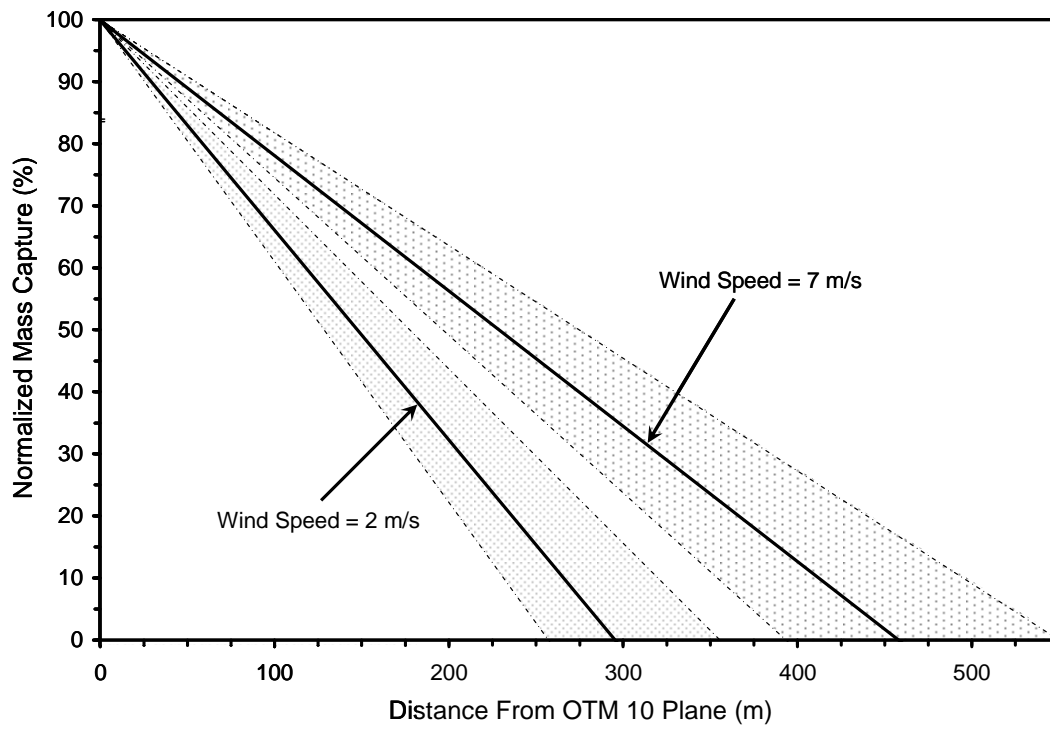


Fig. 6